+ Model
ARTICLE IN PRESS

ELSEVIER

Available online at www.sciencedirect.com
SCIENCE DIRECT®

Sensors and Actuators A xxx (2006) xxx–xxx

SENSORS AND ACTUATORS A PHYSICAL

www.elsevier.com/locate/sna

A micro shear stress sensor based on laterally aligned carbon nanotubes

Steve Tung [a], Husein Rokadia [a,*], Wen J. Li [b]

[a] *Department of Mechanical Engineering, University of Arkansas, Mechanical Engineering, 204 Mechanical Engineering, Dickson Street, Fayetteville, AR 72701, United States*

[b] *Center for Micro and Nano Systems, The Chinese University of Hong Kong, Hong Kong SAR, China*

Received 19 July 2005; received in revised form 23 April 2006; accepted 27 April 2006

Abstract

This paper reports the development of a micro thermal shear stress sensor that utilizes multiwalled carbon nanotubes as the sensing element. The sensor was fabricated by laterally aligning randomly distributed nanotubes into a 360 μm long and 90 μm wide conductive trace between two triangular shaped micro electrodes through the use of a high frequency AC electric field. During operation, the aligned nanotubes are electrically heated to an elevated temperature and surface shear stress is measured indirectly by the amount of convective heat transfer from the heated nanotubes to the surrounding fluid flow.

The nanotube alignment process was primarily controlled by three different phenomena: dielectrophoresis, joule heating, and Brownian motion. Numerical simulations, together with experimental verifications, indicated that a successful alignment could only be realized if: (1) the dielectrophoretic force was positive, (2) the electro-thermal force was also positive, and (3) the dielectrophoretic force was high enough to overcome Brownian motion. The aligned nanotube trace has a room-temperature resistance of 580 Ω, which corresponds to a conductivity of 2.7×10^4 S/m. The absolute temperature coefficient of resistivity ranges from 0.01 to 0.04% $^{\circ}\mathrm{C}^{-1}$. This is about one order of magnitude smaller than the highly doped polysilicon sensing material used in the MEMS micro shear stress sensor. The shear stress sensitivity of the nanotube trace operated at a 3% overheat ratio is found to follow the theoretical sensor power $\propto$ (shear stress)$^{1/3}$ relationship, provided the shear stress level is higher than 0.34 mPa. This result confirms the feasibility of using aligned multi-walled carbon nanotubes as a thermal shear stress sensing material.
© 2006 Elsevier B.V. All rights reserved.

Keywords: Shear stress sensor; Carbon nanotubes; Lateral alignment; Dielectrophoresis

1. Introduction

Flow sensors play an important role in various engineering systems that interact with fluid flows. With the emergence of micro and nano technology, flow sensors capable of accurate fluidic metering at the microscopic scale are also becoming increasingly important. This is particularly the case in microfluidic systems like the micro total analysis system (μTAS) where a large set of biomedical experiments can be carried out much more quickly and sometime more accurately than the traditional laboratory apparatus. The key to a successful μTAS is the capability of sampling and manipulating small but precise amounts of samples, buffers, and reagents in microchannels. To meet this demand, flow sensors chosen for a μTAS must be physically smaller than the microchannels. Furthermore, their sensing mechanism must not allow a large exchange of either momentum or energy between the sensors and the flow in order to avoid flow interference [1].

MEMS is a natural selection for the design of microflow sensors due to its precision fabrication techniques and its compatibility with control electronics. Over the last decade, several different MEMS based flow sensors have been developed for microfluidic applications. Among them is the thermal shear stress sensor which measures flow-imposed surface shear stress based on the amount of convective heat transfer from a heated polysilicon sensing element to the surrounding fluid flow [2]. The thermal shear stress sensor is typically 200 μm × 200 μm in size and the polysilicon sensing element is 150 μm long, 3 μm wide and 0.5 μm thick. The large length-to-width ratio is necessary to ensure sensitivity preference in the direction normal to the length [3]. To minimize conduction heat loss to the substrate, a 0.5 μm deep vacuum cavity is usually included underneath the

* Corresponding author. Tel.: +1 479 871 0033.
E-mail address: huseinrokadia@gmail.com (H. Rokadia).

0924-4247/$ – see front matter © 2006 Elsevier B.V. All rights reserved.
doi:10.1016/j.sna.2006.04.039

sensing element. Experimental results indicated that this unique feature significantly increased the shear stress sensitivity and minimized the sensor's long-time drift [4].

The MEMS thermal shear stress sensor has been proven to be effective in both air [5] and liquid flows [6]. It has also been shown capable of handling biofluids [7]. However, the usage of highly doped polysilicon as the sensing material imposes several severe constraints on the sensor's future development into an effective nanofluidic sensor. Firstly, the polysilicon sensing element is defined by photolithography, which currently has a resolution limit about 100 nm. To handle nanofluids, a much smaller sensing element might be necessary. Secondly, the highly doped polysilicon is a high-temperature material; it requires a 1000 °C annealing step after doping. This behavior has complicated the sensor fabrication process and limited the inclusion of temperature-sensitive materials into the sensor design. Finally, to achieve a reasonable sensitivity, the polysilicon sensor must consume mW range power, which might just be large enough to have an adverse effect on the nanoflow it is intended to sense.

An alternative sensing material must consume less power while maintaining reasonable shear stress sensitivity. According to [8], the shear stress sensitivity of thermal sensors can be maintained at a low power setting by using either a small thermal mass or a sensing material with a large temperature coefficient of resistivity (TCR). The TCR of highly doped polysilicon is around $0.1\%\,°C^{-1}$ and it is therefore desirable for any alternative sensing material to have a comparable or higher TCR. Otherwise, this material must be capable of being scaled down, preferably in a low temperature environment, beyond the polysilicon's 100 nm limit.

2. Carbon nanotubes as flow sensing material

Recent studies have indicated that carbon nanotubes (CNTs) can potentially replace highly doped polysilicon as an alternative thermal shear stress sensing material. CNTs are small cylindrical tubes of graphitically bonded carbon molecules. They exist in two forms: single-walled and multi-walled (Fig. 1). Single-walled nanotubes (SWNTs), typically 1–10 nm in diameter, consist of a single layer of carbon molecules while multi-walled nanotubes (MWNTs), 10–50 nm in diameter, consist of concentric rings of SWNTs. CNTs have a unique electrical property: they can be either metallic of semiconducting depending on the tube diameter and chirality [9]. Such behavior, together with their natural nanometer diameter size, makes CNTs ideally suited for nanoelectronics devices. Recently, MWNTs were found to have a reasonable TCR value [10,11], suggesting the possibility of utilizing MWNTs as a nanoscale shear stress sensing material.

Presently, CNTs can be synthesized by a variety of methods including laser vaporization, carbon arc, and chemical vapor deposition (CVD) [12]. Unfortunately, none of these methods can precisely dictate the physical geometry of the CNTs produced. As a result, CNTs are usually available as a mixture of metallic and semiconducting nanotubes. On the average, most of the SWNTs are semi-conducting while most of the MWNTs are metallic. The bulk electrical conductivity of MWNTs was reported to be approximately 2.2×10^4 S/m [13].

Commercial CNTs are mostly available in the form of randomly distributed 'tangled ropes', with each rope typically consisting of a few tens to a few hundreds of CNTs. To utilize these nanotubes as a flow sensing material, an alignment method must be developed to first untangle the CNT ropes and then regroup the individual CNTs into a high aspect ratio trace similar to the polysilicon sensing element. In the last few years, a CVD based synthesis method has been developed to grow vertically aligned MWNTs in situ on a substrate [14]. However, these nanotubes are not suitable for nanoscale flow sensing because their orientation can potentially cause flow disturbance.

3. Dielectrophoresis of carbon nanotubes

We have developed a micro thermal shear stress sensor using randomly distributed but purified MWNTs obtained from commercial sources. Dielectrophoresis (DEP) was used to align the MWNTs. DEP is a room-temperature process through which uncharged particles, such as CNTs, can be translated in a suspending medium by a non-uniform AC electric field generated between a pair of micro electrodes. Based on [15], the time-averaged dielectrophoretic force, F_{DEP}, acting on the particles, can be expressed as

$$F_{\mathrm{DEP}} = \Gamma \varepsilon_{\mathrm{m}} Re\{F_{\mathrm{CM}}\} \nabla |E_{\mathrm{rms}}|^2 \quad (1)$$

where Γ is a shape factor of the particles, ε_{m} the permittivity of the suspending medium, F_{CM} is the Clausius–Mossotti factor, and E_{rms} is the RMS electric field and $\nabla |E_{\mathrm{rms}}|^2$ is the square field gradient. For particles with a large aspect ratio such as CNTs

$$\Gamma = \frac{\pi}{6} r^2 l \quad \text{and} \quad F_{\mathrm{CM}} = \frac{\varepsilon_{\mathrm{p}}^* - \varepsilon_{\mathrm{m}}^*}{\varepsilon_{\mathrm{m}}^*} \quad (2)$$

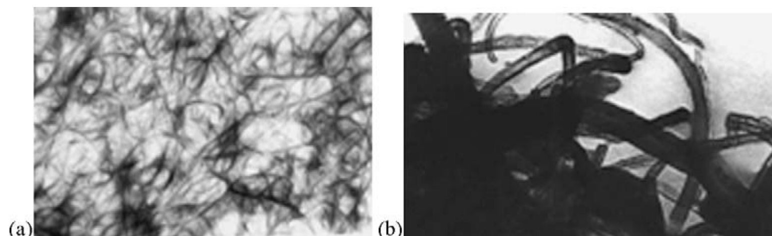

Fig. 1. Transmission electron microscopic (TEM) pictures of carbon nanotubes at 66,000×. (a) Single-walled; (b) multi-walled.

where r is the radius of the particle and l is the length. $\varepsilon^*$is the complex permittivity defined as

$$\varepsilon_m^* = \varepsilon_m^* - i\frac{\sigma_m}{2\pi f}, \quad \varepsilon_p^* = \varepsilon_p - i\frac{\sigma_p}{2\pi f} \tag{3}$$

The subscript p refers to the particle and m refers to the medium. σ is the electrical conductivity, and f is the DEP frequency.

Particles can experience either positive or negative dielectrophoresis depending on the sign of F_{DEP}. If F_{DEP} is positive, particles migrate towards regions of high electric-field gradient. Otherwise, particles move towards regions of low electric-field gradient if F_{DEP} is negative. To realize a high aspect ratio CNT trace in the electrode gap, positive dielectrophoresis can be used in conjunction with a narrow band of high electric field gradient towards which the CNTs can migrate when DEP is initiated. The key is to force the CNTs to align in a preferred direction instead of spreading out across the whole electrode gap.

In addition to being translated by DEP, CNTs in a suspending medium can also be convected by a fluidic motion due to joule heating. Joule heating, a result of the high electric field for DEP, induces a gradient in the conductivity and permittivity of the suspending medium. This in turns leads to an electro-thermal body force F_e on the fluid that can be described by the following equation [16]

$$F_e = -M\left(\frac{\varepsilon_m \sigma_m V_{rms}^4}{2k_T \pi^3 r^3 T}\right)\left(1 - \frac{2\theta}{\pi}\right) \tag{4}$$

where M is a dimensionless factor defined by

$$M = \frac{(T/\sigma_m)(\partial\sigma_m/\partial T) - (T/\varepsilon_m)(\partial\varepsilon_m/\partial T)}{1 + (2\pi f\tau)^2} + \frac{1}{2}\frac{T}{\varepsilon_m}\frac{\partial\varepsilon_m}{\partial T} \tag{5}$$

Here, V_{rms} is the RMS AC voltage, k_T is the suspending medium thermal conductivity, r the radial distance measured from the midpoint of the electrode gap, θ the angle between the plane of the electrodes and a radial line from the midpoint, T the suspending medium temperature, and $\tau = (\varepsilon_m/\sigma_m)$ is the charge relaxation time of the medium. Based on Eq. (4), the magnitude of F_e is the largest at $\theta = 0$ and π, or in a direction parallel to the electrodes. Along this direction, the sign of F_e determines the nature of the fluidic motion with respect to the electrode gap. If F_e is negative, fluid flows into the center of the electrodes, away from the electrode gap. If F_e is positive, fluid flows into the electrode gap from the center of the electrode. To align CNTs in the electrode gap, the fluid must flow in such a way that it brings CNTs into the electrode gap. Because of this, a positive F_e will be desirable.

4. Electric field simulations

Electric field simulations were studied using Ansoft® Maxwell and the results were used to assist in the design of micro electrodes suitable for aligning CNTs. The majority of previous CNT alignment experiments utilized parallel electrodes for DEP. The resulting alignments typically consisted of multiple CNT traces randomly forming across the electrode gap because the electric field distribution is about the same along the gap [17]. Since our interest was in the formation of only a single CNT trace, we chose to use triangular shaped electrodes, with the hope that the DEP effect would be confined to the vicinity of the electrode tips where the electric field was expected to be the strongest. Fig. 2a demonstrates the two-dimensional distribution of the RMS electric field between a pair of triangular shaped electrodes at 3 MHz and 25 V_{p-p}. Each electrode is 260 μm wide and 195 μm long. The tip-to-tip distance is 360 μm. It is clear from the figure that the electric field is indeed the strongest at the electrode tips. Fig. 2b demonstrates the magnitude of $\nabla|E_{rms}|^2$in the electrode gap. Along a line joining the two electrode tips, i.e. the 'Center Line', $\nabla|E_{rms}|^2$is always positive and the highest values are found at the electrode tips. This is unlike the case in parallel electrodes where the highest $\nabla|E_{rms}|^2$ is found along the electrode edge. By using triangular shaped electrodes, DEP effect is confined to a very small area around the electrodes tips. In fact, the size of this area and also the peak $\nabla|E_{rms}|^2$value can be accurately controlled by using different electrode tip angles: the smaller the tip angle, the smaller the DEP region and the higher the $\nabla|E_{rms}|^2$peak.

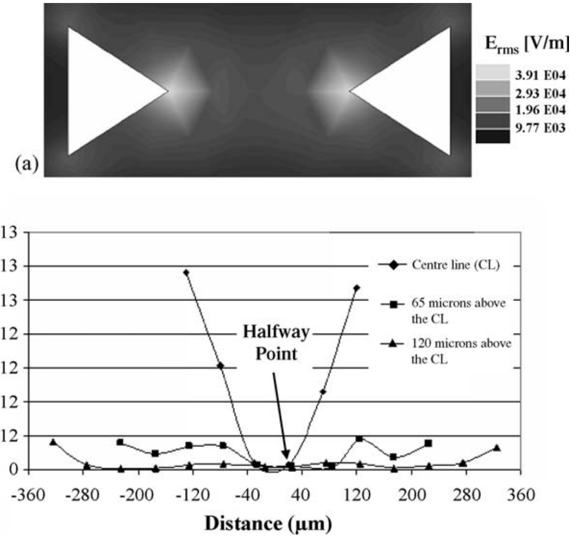

Fig. 2. (a) Simulated rms electric field at 3 MHz and 15 V_{p-p}. (b) Variation of $\nabla|E_{rms}|^2$ along a line between tips of the triangular electrodes. The half-way point indicates the mid-point of the electrode gap.

5. Force calculations

The variation of F_{DEP} with AC frequency is determined based on Eqs. (1)–(3). The highest computed $\nabla|E_{rms}|^2$value at each frequency is used in the calculations. The MWNTs are 20 nm in diameter and 100 μm in length. Their conductivity σ and permittivity ε are assumed to be 2.2×10^4 S/m and $100\varepsilon_0$ F/m, respectively [13]. The suspending medium is DI water with $\sigma = 10^{-3}$ S/m and $\varepsilon = 80\varepsilon_0$ F/m, respectively. As demonstrated in Fig. 3, the variation of F_{DEP} with AC frequency can be described by two plateaus and a continuous varying region. In the low-frequency range between 1 and 10^4 Hz, F_{DEP} is determined mainly by the relative conductivities of the MWNTs and the suspending medium, while in the frequency range between

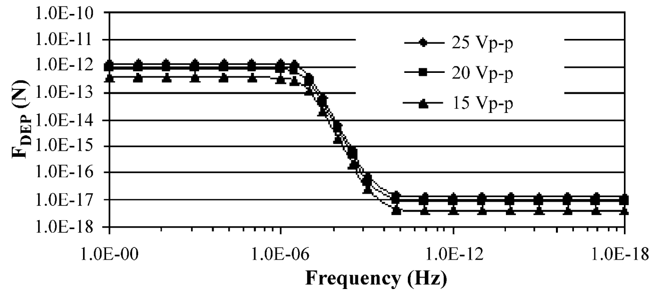

Fig. 3. The dielectrophoretic force as a function of alignment frequency.

10^{10} and 10^{18} Hz, F_{DEP} is controlled by the permittivities. Frequency does not play a major role in either region. Between 10^4 and 10^{10} Hz, frequency can be used to vary F_{DEP} from 10^{-12} to 10^{-17} N. A typical effect of DEP on MWNT migration can be described by considering the case of 3 MHz and 25 V_{p-p}. At this condition, the computed F_{DEP} is approximately 10^{-12} N from Fig. 3. Based on Stokes flow solution for needle-like submerged bodies [18], the velocity of a single MWNT in response to this F_{DEP} should be about 15 μm/s. Since F_{DEP} is positive, the MWNT will migrate towards the triangular electrode tips where the electric field gradient is high. Assuming an initial location of half way between the electrodes, it will take 12 s for the MWNT to travel the 180 μm distance and reach the electrode tip. This result can be considered as a rough time scale for our MWNT alignment using positive DEP.

The variation of F_e at $\theta = 0$ with frequency is determined based on Eq. (4) and shown in Fig. 4. Similar DI water material properties as those used in the F_{DEP} calculations are used. k_T is 0.6 W/(m^2 K) and T is 300 K. Also $(1/\sigma_m)(\partial\sigma_m/\partial T)$ is assumed to be 0.02 °C^{-1}, $(1/\varepsilon_m)(\partial\varepsilon_m/\partial T)$ is −0.004 °C^{-1} [16], and r is 180 μm or half width of the electrode gap. Fig. 4 indicates that F_e, unlike F_{DEP}, is negative at low frequencies and positive at high frequencies. The negative-to-positive transition occurs at approximately 1.4 MHz, which corresponds quite nicely to the relaxation frequency ($=\sigma_m/\varepsilon_m$) of DI water. Assuming that F_e and viscous drag are the only forces acting on the fluid, the fluid velocity should scale with $F_e l^2/\mu$, where l is a length scale and μ is the fluid viscosity. At 3 MHz and 25 V_{p-p}, F_e is 2.3 N/m^3. Substituting l by the half width of the electrode gap, the fluid velocity is approximately 75 μm/s. The fact that the fluid velocity induced by joule heating is of the same order of magnitude as

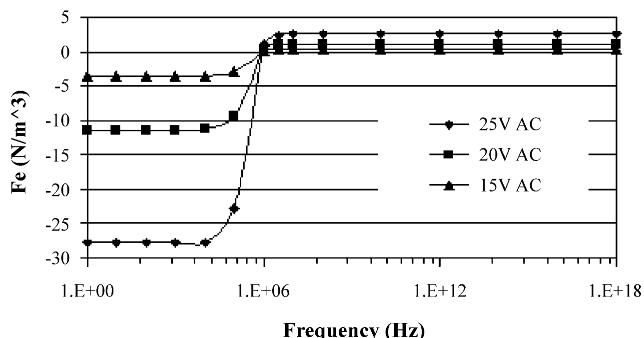

Fig. 4. The electro-thermal force as a function of alignment frequency.

the MWNT velocity induced by F_{DEP} indicates that joule heating must be taken into consideration along with the DEP effect for aligning MWNTs.

Specifically, the frequency chosen for DEP must be higher than 1.4 MHz in order to ensure a positive F_e and a fluid flow direction towards the electrode gap.

6. Alignment results

An experimental study was carried out to align MWNTs between two triangular shaped microelectrodes using DEP. The electrodes were fabricated on a 5 in. glass substrate. The fabrication process involved the deposition of an adhesion layer of 200 Å Cr and a 2000 Å Au electrode layer by sputtering. Photolithography was then used to pattern the metal layer into the desired triangular shape. Each electrode is 260 μm wide at the base and 195 μm long. The two triangles face inward with a tip-to-tip distance of 360 μm. The electrode dimensions are designed to be identical to those used in the numerical simulations.

The MWNT suspension for DEP was prepared by mixing 1 mg of purified MWNTs produced by CVD with 4 mL of DI water and a small drop of Nanosperse®, a poly(oxy-1,2-ethandiyl, an alpha-(nonylphenyl)-omega-hydroxy based surfactant designed to accelerate the dispersion of MWNTs in water. The mixture was sonicated at 44 KHz in a sonic bath until the MWNTs became evenly dispersed in the water. This process usually took 8 to 10 min. Without the Nanosperse®, as long as 4 h was needed to achieve the same degree of MWNT dispersion. Shortening the sonication time not only simplifies the alignment experiment, it also helps to preserve the large aspect ratio of the MWNTs since sonication tends to break the MWNTs into shorter pieces. The MWNT alignment process began with the placement of a 2 μl drop of the MWNT suspension in the electrode gap using an Eppendorf 2100 pipette. Next, an AC potential was applied to the electrodes to generate the required electric field for DEP. The alignment process, as shown in Fig. 5, typically lasts about 2 min, provided the correct AC potential is used. At the beginning, MWNTs precipitate from the suspension drop and align themselves along the electrode edge, as predicted by the numerical simulations. As time elapses, the aligned MWNTs, being mostly metallic, expand the effective area of the alignment electrodes. A direct consequence is a smaller electrode gap and a stronger electric field, which in turn causes more MWNTs to migrate to the electrode tips due to a stronger dielectrophoretic effect. The alignment process continues until two aligned MWNT traces, one from each electrode, link up at the halfway point of the electrode gap, forming a continuous conductive trace. At this point, the AC potential is turned off and the alignment process is terminated.

The width of the aligned MWNT trace typically scales with the size and shape of the electrodes (Fig. 6). When square shaped electrodes are used, the width of the MWNT trace is roughly the same as the electrodes. When triangular shaped electrodes are used, the trace width scales with the tip angle of the electrodes. The MWNT trace shown in Fig. 6b is about 90 μm wide and 0.25 μm thick based on an AFM scan. During the alignment

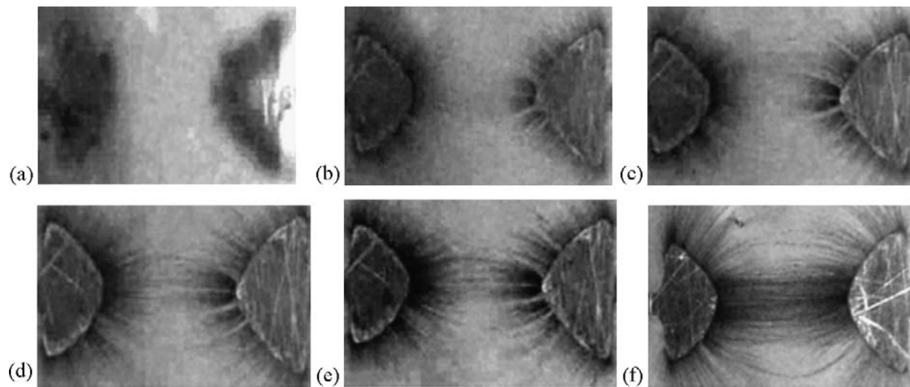

Fig. 5. Sequence of MWNT alignment process. (a) $t = 0$ s, (b) $t = 30$ s (c) $t = 50$ s, (d) $t = 80$ s, (e) $t = 110$ s, and (f) $t = 150$ s.

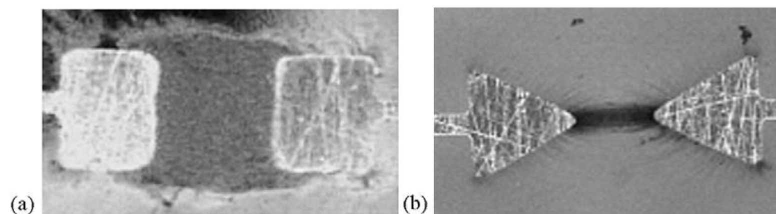

Fig. 6. MWNTs aligned by two different microelectrode shapes.

process, the electrical resistance between the electrodes is continuously monitored. Prior to the linking of the MWNT traces, the resistance is usually in the high MΩ range. As the conductive trace begins to take shape, the resistance begins to decrease until a minimum value of around 1 kΩ is reached.

In the DEP alignment, the DI water in the MWNT suspension is removed through evaporation. As a result, the final aligned MWNT trace is almost 'dry'. However, the electrical properties of a 'freshly' aligned trace are frequently not stable due to the presence of residual water and a poor contact between the MWNTs and the electrodes. Through a 2-h post-alignment annealing at 90 °C, the electrical resistance of the MWNT trace can be stabilized to within ±5%.

Additional DEP experiments were performed to characterize the MWNT alignment under different electric field conditions. In these experiments, the AC potential was varied from 15 to 25 V_{p-p} in increments of 5 V_{p-p} and the alignment frequency was varied from 1 to 3 MHz. At each potential/frequency combination, an alignment process was carried out and the aligned trace evaluated. As shown in Fig. 7, alignment cannot be achieved at 1 MHz, regardless of the potential used. MWNTs at this frequency can be observed to accumulate along the electrode edge, especially at 25 V_{p-p}, indicating a positive DEP. This is in agreement with the F_{DEP} calculations. However, at 1 MHz, F_e is negative, as previously discussed in Section 5, and the fluid motion generated by joule heating flows away from the electrode gap, depleting the MWNTs required to form an aligned trace. When the frequency is raised to 3 MHz, F_e becomes positive and alignment is possible at 20 and 25 V_{p-p}. At 15 V_{p-p}, nanotube alignment fails in the electrode gap, although MWNTs are aligned at the tips and along the electrode edges.

In the case when a MWNT trace is successfully aligned in the electrode gap, additional MWNT streaks also form on the two sides of the alignment electrodes. If the MWNT trace is to be used for flow sensing, these side streaks are undesirable as they compromise the aspect ratio of the trace. By using a sharper

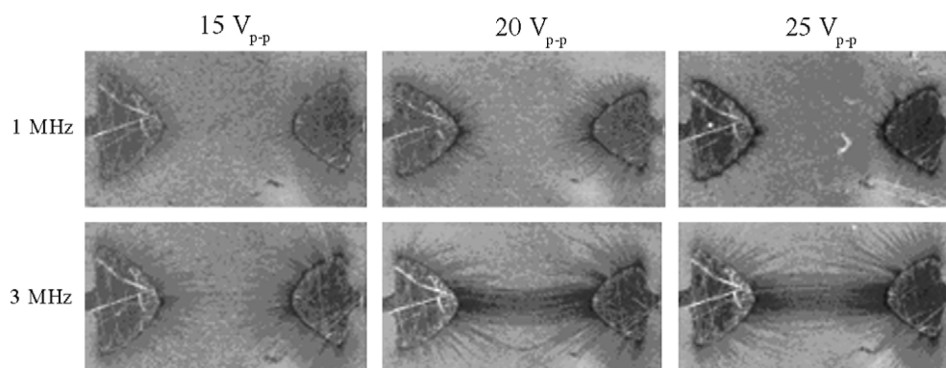

Fig. 7. MWNT alignments under different electric field conditions.

electrode tip together with a lower MWNT concentration in the MWNT suspension, the occurrence of the side streaks can be minimized. Further reduction might require setting up a second electric field by additional electrodes to produce either a counter F_{DEP} or F_e that can force the streaks back into the alignment electrodes.

The results at 3 MHz suggest the presence of a minimum potential for alignment in the case when both F_{DEP} and F_e are positive. It is generally agreed that nanometer scale particle movement due to DEP can only take place if F_{DEP} is larger than the 'disruptive' force caused by Brownian motion. Based on a simple diffusion model [19], the Brownian force was estimated to be $\sim k_B T/2r$ where k_B is the Boltzmann constant. In our alignment experiment where $T = 300$ K and $r = 10$ nm, the Brownian force is $\sim 2.07 \times 10^{-13}$ N. From Fig. 3, F_{DEP} at the electrode tips (where the electric field gradient is the highest) for 3 MHz is about 3.19×10^{-13}, 6.87×10^{-13}, and 10.40×10^{-13} N for 15, 20, and 25 V_{p-p}, respectively. All of them are higher than the Brownian force and MWNTs congregate at the electrode tips as a result. Such is not the case away from the electrode tips where the electric field gradient decreases significantly, as indicated by Fig. 2b. At 15 V_{p-p}, the average $\nabla|E_{rms}|^2$along a line joining the electrode tips is 2.62×10^{12} V^2/m^3 based on the electric field simulations. Substituting this value into Eq. (1), the average F_{DEP} is only 1.81×10^{-13} N. This is smaller than the Brownian force and alignment at 15 V_{p-p} therefore fails. At 20 and 25 V_{p-p}, the average F_{DEP} are 3.33×10^{-13} and 5.21×10^{-13} N, respectively.

7. Electrical properties of aligned MWNT trace

The typical *I–V* characteristics of an annealed MWNT trace are shown in Fig. 8. The linear relationship between the current and applied voltage indicates that the MWNT trace is metallic (within the voltage range tested) with an electrical resistance of 580 Ω. Based on the dimensions of the MWNT trace, the electrical conductivity of aligned MWNTs is determined to be approximately 2.7×10^4 S/m.

The TCR of the MWNT trace was determined by subjecting the trace to a series of temperature changes from 25 to 60 °C.

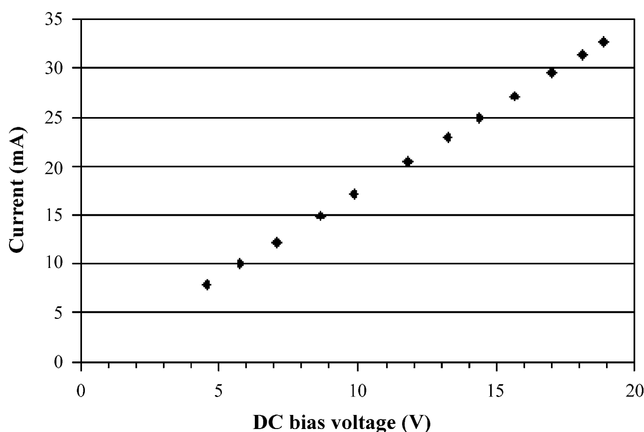

Fig. 8. Typical *I–V* characteristics of annealed MWNT trace.

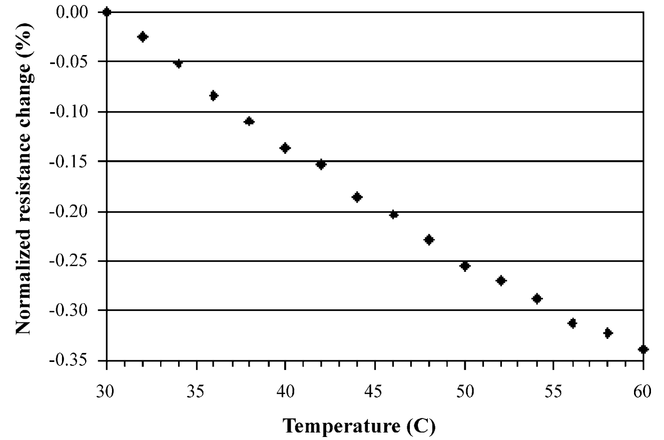

Fig. 9. Electrical resistance variation of MWNT trace with temperature.

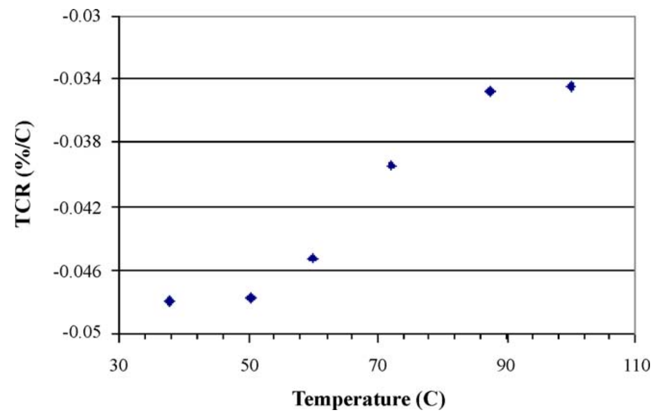

Fig. 10. TCR variation of MWNT trace with temperature.

As demonstrated in Fig. 9, the resistance of the aligned MWNTs varies linearly with temperature at a negative TCR. The absolute TCR value calculated based on several sensors ranges from 0.01 to 0.04 % °C^{-1}. Fig. 10 shows the variation of TCR of one sensor over a wider range of temperature. The typical TCR value of the aligned MWNTs is about one order of magnitude lower than that of the highly doped polysilicon used in the MEMS shear stress sensor and the platinum alloy (80% platinum, 20% iridium) frequently used in the millimeter scale hot wire sensors. The low TCR implies that the shear stress sensitivity of a MWNT trace will be lower than that of a polysilicon trace of similar dimensions operating at the same elevated temperature. For applying MWNTs to shear stress sensor, it therefore only makes sense if a small thermal mass is required as in the case of nanofluidics.

8. Aligned MWNT trace as shear stress sensor

The aligned MWNT trace was tested for shear stress sensitivity in an open-ended Plexiglas channel (2.5 cm wide, 3 mm tall, and 7.5 cm long). It was flush mounted on the channel sidewall at 4 cm downstream from the inlet where laboratory-grade nitrogen gas was fed into the channel as flow medium. Calibration was performed at a flow rate from 10 to 110 sccm. The highest Reynolds number based on channel height and average velocity

was about 300, indicating a laminar flow. Using the established results for laminar duct flows [20], the wall shear stress experienced by the MWNT trace was determined to be in the range from 0.07 to 0.86 mPa.

An external bridge-type constant temperature (CT) circuit commonly used in hot-wire/hot-film anemometry [21] maintained the MWNT trace in a constant temperature mode. The overheat ratio was set at 3%. This corresponds to a sensor operating temperature of about 325 °C, as compared to a typical operating temperature of about 125 °C for the polysilicon shear stress sensor. In a CT mode, the differential voltage output of the CT circuit ΔV scales with the amount of convective heat transfer from the heated MWNT trace to the surrounding flow [22]. The relationship between ΔV and the surface shear stress τ_w for laminar flows can be described by basic heat transfer principles as,

$$\frac{(\Delta V)^2}{R} = A\tau_w^{1/3} + B \qquad (6)$$

where R is the resistance of the MWNT trace and A is a fluid related constant. B is the amount of conductive heat loss from the MWNT trace to the substrate. Since it is not related to τ_w, B must be kept low for the shear stress sensor to be sensitive to convective heat transfer. Unlike the polysilicon shear stress sensor, the MWNT trace does not have a micro cavity underneath. As a result, the operating temperature was intentionally kept low in order to avoid a large B.

By nature, thermal shear stress sensors are susceptible to variations in the environmental temperature. Prior to the flow test, the MWNT shear stress sensor, while maintained at a constant temperature, was tested for temperature sensitivity in an environmental chamber. As indicated by Fig. 11, ΔV of the MWNT shear stress sensor scales mostly linearly with the environmental temperature. Using the slope of the temperature sensitivity line, the ΔV obtained in the subsequent flow test was properly adjusted to compensate for any temperature instability during the test.

Results of the flow test are shown in Fig. 12 in the form of normalized $\Delta V^2/R$ versus $\tau_w{}^{1/3}$. In the $\tau_w{}^{1/3}$ range from 0.0 to 0.6 mPa$^{1/3}$, the MWNT shear stress sensor shows very little sensitivity. This behavior is similar to that of a polysilicon shear stress sensor when the convective heat transfer from the sensor to the fluid flow is not the dominant heat transfer mode and a large portion of the heat generated by the sensor is lost to the substrate. As $\tau_w{}^{1/3}$ exceeds the level of 0.7 mPa$^{1/3}$ ($\tau_w = 0.34$ mPa), the sensor voltage output responds quite nicely to the changing τ_w. In fact, beyond this shear stress level, $\Delta V^2/R$ varies almost linearly with $\tau_w{}^{1/3}$. Judging from this behavior, it can be concluded that the MWNT trace can indeed be used as a thermal shear stress sensing element, provided the shear stress level is above 0.34 mPa or a flow rate of 44 sccm.

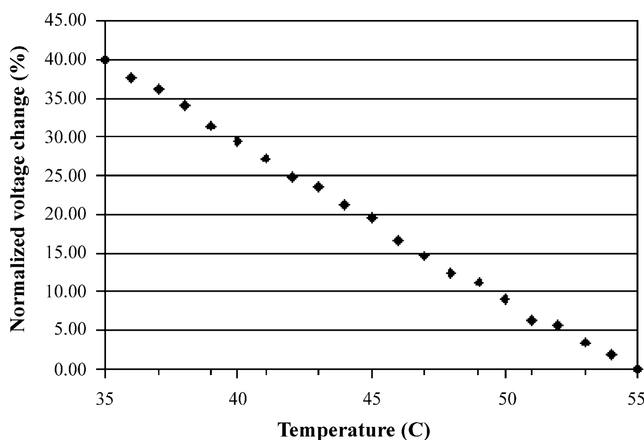

Fig. 11. Variation of MWNT shear stress sensor voltage output with temperature.

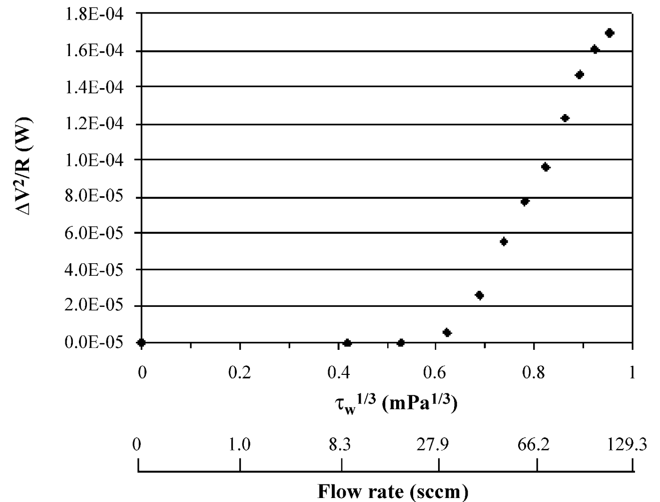

Fig. 12. Variation of MWNT shear stress sensor power with wall shear stress ($\tau_w^{1/3}$) and flow rate.

9. Concluding remarks

We have developed a micro thermal shear stress sensor with aligned MWNTs as the sensing material. The MWNTs, obtained in a randomly oriented form, were aligned between two triangular shaped microelectrodes into a 360 μm long and 90 μm wide conductive trace using a high frequency AC potential applied to the electrodes. The alignment process was dominated by three different phenomena: dielectrophoresis, joule heating, and Brownian motion. Numerical simulations together with experimental alignment results indicated that three conditions must be met for an aligned MWNT trace to be realized: a positive dielectrophoretic force, a positive electro-thermal force, and a high enough dielectrophoretic force to overcome Brownian motion.

The aligned MWNT trace behaves as a thermistor with a nominal resistance of 580 Ω at room temperature. Its absolute TCR value ranges from 0.01 to 0.04% °C^{-1}, which is about one order of magnitude smaller than heavily doped polysilicon. This result suggests that the MWNT shear stress sensor is better suited for an environment where a small thermal mass is required. The MWNT trace was calibrated for shear stress sensitivity in a millimeter size wind tunnel while operated in a constant temperature mode. The calibration result shows a one-third power relationship between the sensor power output and wall shear stress, indicating a true shear stress sensor behavior in the MWNT trace.

The MWNT trace described in the present paper is of μm scale. Because of this, it will be more suitable for microfluidic instead of nanofluidic applications. To realize a nanometer scale trace, a nanometer electrode gap size together with two extremely sharp electrode tips will be required. The gap size is controlled by the capability of photolithography which has a current resolution of about 100 nm. The sharp tips will limit the width of the trace to about tens of nanometers, according to our latest alignment results (not reported in this paper). We believe the alignment of a single bundle of CNTs consisting of about ten individual nanotubes is possible. If this is indeed the case, by carefully selecting the right kind of CNTs, a thermal shear stress sensor of 100 nm long and 10 nm wide should be realizable.

Acknowledgements

This project is partially supported by NSF (#ECS-0220850), the Hong Kong Research Grant Council (CUHK 4177/04E), and also the Shun Hing Institute of Advanced Engineering (BME-3/05).

References

[1] C.M. Ho, Y.C. Tai, Micro-electro-mechanical-systems (MEMS) and fluid flows, Annu. Rev. Fluid Mech. 30 (1998) 579–612.
[2] C. Liu, J.-B. Huang, A.Z. Zhu, F. Jiang, S. Tung, Y.-C. Tai, C.-M. Ho, A Micromachined flow shear stress sensor based on thermal transfer priciples, J. Microelectromech. Syst. 8 (1999) 90–99.
[3] R.J. Goldstein, Fluid Mechanics Measurements, Hemisphere Publishing Corp., New York, 1983, p. 161.
[4] J. Huang, S. Tung, C.M. Ho, C. Liu, Y.C. Tai, Improved micro thermal shear-stress sensor, IEEE Trans. Instrum. Meas. 45 (1996) 570–574.
[5] S. Tung, B. Maines, F. Jiang, T. Tsao, Development of a MEMS-based control system for compressible flow separation, J. Microelectromech. Syst. 13 (2004) 91–99.
[6] Y. Xu, J. Clendenin, S. Tung, F. Jiang, Y.-C. Tai, Underwater flexible shear stress sensor skins, in: Proceedings of IEEE International MEMS-04 Conference, Maastricht, Netherlands, January 25–29, 2004.
[7] G. Soundararajan, T.K. Hsiai, L. DeMaio, M. Chang, S. Chang, MEMS shear stress sensor for cardiovascular diagnostics, in: Proceedings of the 26th Annual International Conference of the IEEE EMBS, San Francisco, CA, September 1–5, 2004.
[8] K. Breuer, MEMS Sensors for Aerodynamic Applications, Proceedings of the 38th Aerospace Sciences Meeting & Exhibit, AIAA paper 2000-0251, Reno, NV, January 10, 13, 2000.
[9] C.L. Kane, E.J. Mele, Size, shape, and low energy electronic structure of carbon nanotubes, Phys. Rev. Lett. 78 (1997) 1932–1935.
[10] J. Clendenin, H. Rokadia, S. Tung, K. Ogburia, Application of aligned carbon nanotubes in micro shear stress sensing, in: Proceedings of the International Mechanical Engineering Congress and RD&D Expo, IMECE2004-61227, Anaheim, CA, November 13–19, 2004.
[11] C.K. Fung, V. Wong, R. Chan, W.J. Li, Dielectrophoretic Batch Fabrication of Bundled Carbon Nanotube Thermal Sensors, IEEE Trans. Nanotechnol. 3 (2004) 395–403.
[12] R. Saito, G. Dresselhaus, M.S. Dresselhaus, Physical Properties of Carbon Nanotubes, Imperial College Press, London, 1999, p. 150.
[13] C.A. Grimes, C.E.C. Dickey, C. Mungle, K.G. Ong, D. Qian, Effect of purification of the electrical conductivity and complex permittivity of multi wall carbon nanotubes, J. Appl. Phys. 90 (2001) 4134–4137.
[14] Z. Ren, Z. Huang, J. Xu, J. Wang, P. Bush, M. Siegal, P. Provencio, Synthesis of large arrays of well-aligned carbon nanotubes on glass, Science 282 (1998) 1105–1107.
[15] M. Dimaki, P. Boggild, Dielectrophoresis of carbon nanotubes using microelectrodes: a numerical study, Nanotechnology 15 (2004) 1–8.
[16] A. Ramos, H. Morgan, N. Green, A. Castellanos, AC electrokinetics: a review of forces in microelectrode structures, J. Phys. D: Appl. Phys. 31 (1998) 2338–2353.
[17] J. Chung, K.-H. Lee, J. Lee, Microfabricated glucose sensor based on single-walled carbon nanotubes, in: Proceedings of IEEE International MEMS-04 Conference, Maastricht, Netherlands, January 25–29, 2004.
[18] F.M. White, Viscous Fluid Flow, New York, McGraw Hill, 1991, p. 280.
[19] H.A. Pohl, Dielectrophoresis, Cambridge University Press, Cambridge, UK, 1978, p. 171.
[20] F.M. White, Viscous Fluid Flow, McGraw Hill, New York, 1991, p. 200.
[21] J. Clendenin, M. Gordon, S. Tung, Pressure sensitivity of a thermal shear stress sensor, in: Proceedings of FEDSM'03 4TH ASME–JSME Joint Fluids Engineering Conference, Honolulu, HI, July 6–11, 2003.
[22] Y. Xu, Y.-C. Tai, F. Jiang, Q. Lin, J. Clendenin, S. Tung, Underwater shear stress sensor, in: Proceedings of IEEE International MEMS-02 Conference, Las Vegas, NV, January 20–24, 2002.

Biographies

Steve Tung received his BS degree from the National Taiwan University in 1984 and his PhD degree in mechanical engineering from the University of Houston in 1992. From 1993 to 1997, he was a postdoctoral Fellow at the Department of Mechanical and Aerospace Engineering at UCLA where he worked on the development of a MEMS based shear stress sensor. From 1997 to 1999, he was a MEMS Engineering Specialist at Litton Guidance and Control Systems, Woodland Hills, CA. In January 2000, he joined the Department of mechanical engineering of the University of Arkansas, Fayetteville, where he is currently an associate professor. Prof. Tung's research interests are mainly in the area of micro and nano technologies for biological and biomedical applications. He has served as the principal investigator of a wide variety of research projects funded by NSF, NASA, DOT, USDA, and ONR.

Husein Rokadia received his BE from the University of Mumbai, India, in 2000 and his MS degree in Mechanical Engineering from University of Arkansas, USA, in 2004. He is currently a PhD candidate in Mechanical Engineering under the council of Dr. Steve Tung at the University of Arkansas. His research interests include BioMEMS and bio nanotechnology.

Wen J. Li received the BS and MS degrees in Aerospace Engineering from University of Southern California (USC) in 1987 and 1989, respectively. He obtained his PhD degree from University of California, Los Angeles (UCLA) in 1997 specializing in MEMS. He received the Aerospace Corporate Fellowship, Silicon Microstructures Inc., Employee Award, and a NASA technical innovation award for his technical contributions to those organizations. Prof. Li joined the Department of Automation and Computer-Aided Engineering in 1997. He has since then been active in MEMS and nanotechnology research. In the past 6 years he has published more than 110 papers in professional journals and conference proceedings on MEMS and nanotechnology related work.